This Page Is Inserted by IFW Operations
and is not a part of the Official Record

BEST AVAILABLE IMAGES

Defective images within this document are accurate representations of the original documents submitted by the applicant.

Defects in the images may include (but are not limited to):

- BLACK BORDERS

- TEXT CUT OFF AT TOP, BOTTOM OR SIDES

- FADED TEXT

- ILLEGIBLE TEXT

- SKEWED/SLANTED IMAGES

- COLORED PHOTOS

- BLACK OR VERY BLACK AND WHITE DARK PHOTOS

- GRAY SCALE DOCUMENTS

IMAGES ARE BEST AVAILABLE COPY.

As rescanning documents *will not* correct images, Please do not report the images to the Image Problem Mailbox.

(12) INTERNATIONAL APPLICATION PUBLISHED UNDER THE PATENT COOPERATION TREATY (PCT)

(54) Title: ADAPTIVE CALIBRATION PULSED OXIMETRY METHOD AND DEVICE

(57) Abstract: A method for determining an arterial blood oxygen saturation level according to this invention includes measuring the light transmittance through tissue of light of a first wavelength, and a second wavelength (20). A steady-state component of the measured light transmission is used to select an appropriate calibration curve (30). A pulsatile component of the measured light transmission is used to determine the arterial blood oxygen saturation level using the selected calibration curve (40). An oximetry system is also provided.

ADAPTIVE CALIBRATION PULSED OXIMETRY METHOD AND DEVICE

This application claims priority from U.S. Provisional Patent Application Serial No. 60/143,894, which is incorporated herein by reference.

BACKGROUND OF THE INVENTION

This invention relates generally to oximeters that measure arterial blood oxygen saturation (S_aO_2) levels in tissues. More specifically, this invention relates to oximeters that use the pulsatile component of light of multiple wavelengths to determine the amount of arterial blood oxygen saturation.

The arterial blood oxygen saturation and pulse rate of an individual are of interest for a variety of reasons. For example, emergency or surgical care settings can use information regarding oxygen saturation to signal changing physiological factors, the malfunction of anesthesia equipment, or physician error. Similarly, in the intensive care unit, oxygen saturation information can be used to confirm the provision of proper patient ventilation or to optimize a gradual reduction and eventual removal from assisted ventilation.

The proper utilization of many lifesaving medical techniques and treatments depends upon the attending physician continually obtaining accurate and up-to-date information regarding various bodily functions of the patient. Heart rate, blood pressure, and arterial oxygen saturation are among the most critical information that a physician needs to determine an optimal course of treatment. Continuous provision of this information is crucial to allow the physician to immediately adopt a procedural course that will best meet a patient's needs.

Arterial oxygen saturation (S_aO_2) is expressed as a percentage ratio of hemoglobin which is bound to oxygen (i.e., oxygenated hemoglobin (HbO_2 or "oxyhemoglobin")) to the total hemoglobin in the patient's blood (including both oxygenated (HbO_2) and non-

1

oxygenated hemoglobin (Hb)), as represented by the following equation:

$$S_aO_2 = ([HbO_2]/([Hb]+[HbO_2])) \times 100\%$$

In a healthy patient, the S_aO_2 value is generally above 95% since blood traveling through the arteries has just passed through the lungs and has been oxygenated. As blood courses

5　through the capillaries, however, oxygen is off-loaded into the tissues and carbon dioxide is on-loaded into the hemoglobin. Thus, the oxygen saturation levels in the capillaries (S_cO_2) is always lower than in the arteries. Once the blood has provided oxygen to the body tissue, the blood returns to the heart through the veins. Accordingly, the blood oxygen saturation levels in the veins is even lower still (i.e., about 75%).

10　　　　Importantly, if the patient's arterial oxygen saturation level is too high or too low, the physician can take corrective action, such as reducing or increasing the amount of oxygen being administered to the patient, only after he or she learns of the incorrect saturation level. Proper management of arterial oxygen saturation is particularly important in neonates where S_aO_2 must be maintained high enough to support cell

15　metabolism but low enough to avoid damaging oxygen-sensitive cells in the eye, which could cause impairment or complete loss of vision. Accordingly, in many applications, the continual provision of up-to-date information regarding the patient's pulse rate and oxygen saturation level is crucial to allow the physician to detect harmful physiological conditions before any observable physical manifestations of a substantial risk of injury

20　arise. In settings such as operating rooms and in intensive care units, monitoring and recording these indicators of bodily functions is particularly important. For example, when an anesthetized patient undergoes surgery, it is generally the anesthesiologist's role to monitor the general condition of the patient while the surgeon proceeds with his tasks.

　　　　Typical techniques for measuring these characteristics include invasive

25　procedures, such as using an inserted catheter to measure blood pressure and to extract periodic blood samples, or non-invasive techniques. Unfortunately, although invasive procedures are typically more accurate than non-invasive ones, they generally take several minutes to obtain results. These wasted minutes can be crucial in many medical situations as human tissue can begin to degenerate with lack of sufficient oxygen in just a

few minutes. Non-invasive techniques are therefore generally preferred, not only because they avoid the painful insertion of needles or other instrumentation into a patient's body, but also because they offer a quicker response to changing physiological characteristics of the patient. Noninvasive techniques are also desirable when complex blood diagnostic

5   equipment is not available, such as, for example, when a home health care provider performs a routine check-up in a patient's home.

The term "oximetry" has been adopted in the art to refer to noninvasive apparatus and methods for determining blood oxygen saturation levels. Conventional types of oximeters include finger oximeters, earlobe oximeters, and fetal oximeters. Conventional

10   oximetry systems make use of the fact that the absorption characteristics of different blood components, namely, HbO_2 and Hb, differ depending on which wavelength of light (e.g., infrared or visible portions of the spectrum) is being used. Accordingly, typical noninvasive oximetric systems impinge at least both visible and infrared light upon a body part, such as a finger, and then estimate the S_aO_2 level using the relative proportions

15   of visible and infrared light transmitted through or reflected by the body tissue. Undesirably, however, these conventional systems inherently include some inaccuracy, which increases to a substantial error for low (50-70%) S_aO_2 levels, due to, among other things, the inclusion of capillary blood as well as arterial blood in the light measurement readings.

20   In an effort to improve the accuracy of the S_aO_2 values obtained using two wavelengths of light, some systems have utilized the pulsatile component of the transmitted or reflected light beam to distinguish variations in the detected intensity of the light beam which are due to changes in blood components from other causes. This approach is generally referred to as pulse oximetry. Using the pulsatile signal modulating

25   the light beams for obtaining an S_aO_2 estimate provides a significant improvement in accuracy over non-pulse oximetry systems.

"Pulsed oximeters" are therefore oximeters which measure the arterial component of the blood perfusion, to yield the arterial oxygen saturation (S_aO_2) level, using the pulsatile component of a light transmission signal. Companies have built special circuitry

3

and developed algorithms to obtain good signal-to-noise ratios for this pulsatile

measurement. These conventional circuits and algorithms typically yield a pulsatile

factor (R) which is based in part on the ratio of the pulsatile component of light

measurements at a red wavelength (eg., 600-800 nm) and at an infrared wavelength (eg.,

5   800-1000 nm). More specifically, the pulsatile factor R is equal to a ratio of the pulsatile

component divided by the steady-state component of light at the red wavelength to the

pulsatile component divided by the steady-state component of light at the infrared

wavelength, as shown by the equation:

$$R = (AC/DC)_{red}/(AC/DC)_{infrared}$$

10   The pulsatile factor R therefore properly corrects for variation in the power of the

light sources and photodetectors comprising the measurement device. As will be

discussed later, the ratio R does not, however, correct for the background tissue optics

consisting of tissue thickness, tissue blood perfusion, light scattering, and boundary

conditions such as bones and the air/tissue surface.

15   As explained above, traditional oximeters calibrate their pulsatile factor R

measurement using non-invasive light transmission or reflection analysis as opposed to

direct measurement of arterial S_aO_2 measured with catheters inserted in arterial vessels.

More specifically, pulse oximeters monitor blood oxygen content by measuring the

absorption of light in an arterialized vascular bed. Since oxyhemoglobin (HbO_2) and

20   deoxyhemoglobin (Hb) absorb light differently, the relative concentration of each blood

component and thus the S_aO_2 can be determined by measuring absorbed light at two

different wavelengths. Pulse oximetry is now an established standard of care during

anesthesia and in neonatal and adult critical care.

The basic design of conventional pulse oximeter probes includes both red and

25   infrared light emitting diodes (LEDs) and a photodetector (or light transducer). These

components are arranged so that the LEDs illuminate a particular section of arterialized

tissue. The detector collects the light from the LEDs which has been transmitted through

the tissue section but not absorbed by the skin, bone, blood and other physiologic

4

absorbers. The steady-state (DC) and time-varying (AC) components of this signal are then used to calculate the fraction of the arterial blood which is oxygenated.

Pulse transmittance oximetry basically involves measurement of how the arterial blood in body tissue affects the intensity of light passing therethrough. More particularly,

5   the volume of blood in the tissue is a function of the arterial pulse, with a greater volume present at systole and a lesser volume present at diastole. Because blood absorbs some of the light passing through the tissue, the intensity of the light emerging from the tissue is inversely proportional to the volume of blood in the tissue. Thus, the emergent light intensity will vary with the arterial pulse and can be used to indicate a patient's pulse rate.

10   In addition, the absorption coefficient of HbO_2 is different from that of Hb for most wavelengths of light. For that reason, differences in the amount of light absorbed by the blood at two different wavelengths can be used to indicate the level of arterial oxygen saturation, S_aO_2. Thus, by measuring the amount of light transmitted through an earlobe or finger, for example, a pulse oximeter can be used to determine both the patient's pulse

15   rate and arterial blood oxygen saturation.

The intensity of light transmitted through an earlobe, finger, or other body part is a function of the absorption coefficient of both "fixed" and "variable" components. Examples of "fixed" components include bone, tissue, skin, and hair. Examples of "variable" components include the volume of blood in the tissue. The intensity of light

20   transmitted through the tissue is generally expressed as a function of time. It includes a baseline (or "DC") component, which varies slowly with time and represents the effect of the fixed components on the light transmission. It further includes a periodic pulsatile (or "AC") component, which varies more rapidly with time and represents the effect that changing tissue blood volume has on the light. Because the attenuation produced by the

25   fixed tissue components does not contain information about pulse rate and arterial oxygen saturation, the pulsatile signal is of primary interest. In that regard, many of the transmittance oximetry techniques of the prior art eliminate the baseline component from the signal analyzed.

For example, U.S. Pat. No. 2,706,927 (Wood) measures light absorption at two

wavelengths under a "bloodless" condition and a "normal" condition. In the bloodless condition, as much blood as possible is squeezed from the tissue being analyzed. Then, light at both wavelengths is transmitted through the tissue and absorption measurements made. These measurements indicate the effect that all non-blood tissue components have

5   on the transmission of light through the tissue. When normal blood flow has been restored to the tissue, a second set of measurements is made that indicates the influence of both blood and non-blood components. The difference in light transmission measurements between the two conditions is then used to determine the average oxygen saturation of the tissue, including the effects of both arterial and venous blood. This

10   process essentially eliminates the DC, non-blood component from the signal used to determine oxygen saturation.

For a number of reasons, however, the Wood method fails to provide the necessary accuracy. For example, a true bloodless condition cannot be obtained practically. In addition, efforts to obtain a bloodless condition, such as by squeezing the

15   tissue, may result in a different light transmission path for the two conditions. In addition to problems with accuracy, the Wood approach is both inconvenient and time consuming and can cause damage to the tissue.

A more refined approach to pulse transmittance oximetry is disclosed in U.S. Pat. No. 4,086,915 (Kofsky et al.). The Kofsky et al. patent is of interest for two reasons.

20   First, the technique of Kofsky et al. automatically eliminates the effect that fixed components in the tissue have on the light transmitted therethrough, avoiding the need to produce bloodless tissue. More particularly, as developed from the Beer-Lambert law of absorption for a clear medium with no light scattering, the derivatives of the intensity of the light transmitted through the tissue at two different wavelengths, when multiplied by

25   predetermined pseudo-coefficients, can be used to determine oxygen saturation. Basic mathematics indicates that such derivatives are substantially independent of the DC component of the intensity, however the simple math does not hold for an optically turbid medium such as tissue with strong light scattering. The pseudo-coefficients are determined through measurements taken during a calibration procedure in which a patient

6

first respires air having a normal oxygen content and, later, respires air of a reduced oxygen content. Unfortunately, this process is cumbersome.

Another reference addressed to pulse transmittance oximetry is U.S. Pat. No. 4,407,290 (Wilber). According to Wilber, light pulses produced by LEDs at two different

5   wavelengths are applied to a body part, such as an earlobe. A sensor responds to the light transmitted through the earlobe, producing a signal for each wavelength having a DC and AC component resulting from the presence of constant and pulsatile absorptive components, respectively, in the earlobe. A normalization circuit employs feedback to scale both signals so that the DC, non-pulsatile components of each are equal and so that

10   these offset voltages can be removed. Decoders separate the two signals, so controlled, into channels A and B where the DC component is removed from each. The remaining AC components of the signals are amplified and combined in a multiplexer prior to analog-to-digital (A/D) conversion. Oxygen saturation is then determined by a digital processor.

15   European Patent Application No. 83,304,939.8 (New, Jr. et al.) discloses yet another pulse transmittance oximeter. According to New, Jr. et al., two LEDs expose a body member, such as a finger, to light having red and infrared wavelengths, with each LED having a one-in-four duty cycle. A detector produces a signal in response to the light that is split into two channels. The one-in-four duty cycle allows negatively

20   amplified noise signals to be integrated with positively amplified signals including the detector response and noise, thereby eliminating the effect of noise on the signal produced. The resultant signals include a substantially constant DC component and an AC component. To improve the accuracy of a subsequent analog-to-digital (A/D) conversion, a fixed DC value is subtracted from the signal prior to the conversion. This

25   level is then added back in by a microprocessor after the conversion. Logarithmic analysis is avoided by the microprocessor because for each wavelength of light transmitted through the finger, a quotient of the AC component over the constant DC component is determined. The ratio of the two quotients is then determined and fitted to a curve of independently derived oxygen saturation levels. To compensate for the

different transmission characteristics of different patient's fingers, an adjustable drive source for the LEDs is provided.

Pulsed oximetry has been successful as a trend detector to detect a sudden fall in S_aO_2 from the normal value of approx. 95%. However, pulsed oximetery has failed to prove accurate over a broad range of saturation levels. The subject-to-subject and tissue site-to-site variation in tissue blood perfusion is too great to allow a single calibration curve to relate R to S_aO_2 for all cases. Pulsed oximetry needs adaptive calibration to properly interpret R values based on pulsatile light transmission to yield accurate S_aO_2 values. There is a significant need for an oximeter with adaptive calibration.

SUMMARY OF THE INVENTION

One object of the present invention is to enable a method of determining an arterial blood oxygen saturation level that is accurate over various oxygen saturation levels.

Another object of the present invention is to enable a method of determining an arterial blood oxygen saturation level that is adaptively calibrated to give accurate blood oxygen saturation values over a range of oxygen saturation levels.

The present invention is an oximetry system that uses a plurality of sets of calibration curves, each containing a plurality of calibration curves, to permit accurate calibration of the system over a range of oxygen saturation levels.

According to the invention, an adaptively calibrated pulse oximeter uses the steady-state component of light transmission measurements to select a proper calibration curve. The selected calibration curve is then used to properly interpret the pulsatile factor obtained from the conventional measurement of the pulsatile component of the light signals to yield an accurate arterial blood oxygen saturation level determination.

In general, one method of determining an arterial oxygen saturation level according to this invention proceeds by using the DC components of light transmission measurements for both red and infrared light to determine a blood volume fraction/mixed blood oxygen saturation value pair. The unique pair is then used to select an appropriate calibration curve. Once the appropriate calibration curve has been selected, a pulsatile

factor can then be used to determine the corresponding arterial blood oxygen saturation value.

More specifically, light measurements at the red and infrared wavelengths are taken with the probe in air (or some other standard medium). These calibration

5   measurements are one-time measurements to allow correction for variation in the power of the light source and for variation in the responsivity of the detector. Subsequent measurements of the tissue are normalized by the calibration measurements. The normalized measurements are then used to determine the volume fraction of blood in the tissue and the mixed blood oxygen saturation value from a grid mapping. An appropriate

10   calibration curve from among a plurality of calibration curves can then be selected using the blood volume fraction and the mixed blood oxygen saturation value.

According to one embodiment, a plurality of sets of calibration curves can also be provided. Each set of calibration curves includes a plurality of calibration curves relating the pulsatile factor to the arterial blood oxygen saturation level. The volume blood

15   fraction and the mixed blood oxygen saturation value are used to select an appropriate calibration curve from among the plurality of calibration curves. Using the appropriate calibration curve, the pulsatile factor can be properly interpreted to yield an arterial blood oxygen saturation value. If the blood volume fraction or mixed blood oxygen saturation value of the patient's tissue site changes, the calibration will change accordingly to

20   adaptively calibrate the determination of arterial blood oxygen saturation values.

BRIEF DESCRIPTION OF THE DRAWINGS

The foregoing objects, features, and advantages of the present invention will become more readily apparent from the following detailed description of multiple embodiments

25   thereof, made with reference to the following figures, in which:

FIG. 1 is a schematic flow diagram illustrating a method of determining an arterial blood oxygen saturation level according to one embodiment of the present invention.

FIG. 1A is a schematic system level diagram illustrating an oximetry system for implementing the method of FIG. 1 according to another embodiment of the present

9

invention.

FIG. 2 is a block flow diagram illustrating a basic algorithm for determining the arterial blood oxygen saturation level according to the method illustrated in FIG. 1.

FIG. 3 is a grid showing a relationship between light transport factors and blood volume fraction and mixed blood oxygen saturation values as used in the method illustrated in FIG. 1.

FIG. 4 is a graph showing a set of calibration curves for a given mixed blood oxygen saturation value for use in the method illustrated in FIG. 1.

FIG. 5 is a listing of a calibration program for generating calibration curves for use in the method illustrated in FIG. 1.

FIG. 6 is a listing of a subroutine for calculating a pulsatile factor R for use in the calibration program of FIG. 5.

FIG. 7 is a graph showing calibration factors calculated for use in the method illustrated in FIG. 1.

FIG. 8 is a program listing of a program for calculating calibration factors for use in the method illustrated in FIG. 1.

FIG. 9 is a program listing of a computer program for generating the grid mapping of FIG. 3.

FIG. 9A is a program listing of a subroutine for use in the program of FIG. 9.

DETAILED DESCRIPTION

Like the prior art, the method and apparatus of this invention can be used to monitor blood oxygen saturation in the emergency room, in surgery, in intensive care, in the neonatal intensive care unit, monitoring the fetus during child birth, and in home use for monitoring peripheral vascular disease, among other uses. As noted previously, pulse oximeters measure the pulsatile change in transmission of light through a tissue due to the pulsatile change in tissue blood content caused by the beating heart. Such pulsatile measurements are generally made at two wavelengths (red and infrared) which are combined to yield a pulsatile factor R that is directly related to the arterial blood oxygen

saturation value, S_aO_2. Accordingly, by measuring R, the S_aO_2 can be determined.

Unfortunately, however, the calibration curve which maps an R value to an S_aO_2 value is not constant. The calibration curve of R versus S_aO_2 will vary from patient to patient and from tissue site to tissue site. The key factor underlying the failure of the

5   prior art is the reliance of previous methods on the assumption of Beer's Law to describe light transport in tissue. Beer's Law would be appropriate if tissue were a cuvette of clear hemoglobin solution such that the tissue was transparent with no light scattering to cause optical turbidity. In such a case, the current calibration curves of R versus S_aO_2 would be accurate. Tissue turbidity due to light scattering, however, causes the light transport

10   problem to become nonlinear, and the simple calculation of R consequently does not correct for the background tissue optics. The time-averaged blood content, both arterial and venous, influences the transport of light through the tissue and hence influences the calibration curve of R versus S_aO_2. Proper interpretation of the pulsatile (AC) component of light transmission to yield S_aO_2 requires a calibration that depends on the baseline

15   (DC) component of light transmission.

In simple terms, consider dropping a drop of blood into a cup of milk and into a cup of milk plus coffee. In which cup would the color of the added blood be more pronounced? The color is more pronounced in the cup of milk than in the cup of milk plus coffee. In this analogy, the coffee mimics the time-averaged blood content, both

20   arterial and venous, that influences the transport of light through the tissue. The added blood mimics the pulsatile increase in blood content of a tissue during the heart beat. To judge the amount of added blood by the color of blood in each cup one must account for the background optics (i.e., with or without coffee). The amount of coffee will vary the calibration curve required to deduce the amount of added blood from the color of blood in

25   each cup. The judgment of the amount of added blood in the cup is analogous to deducing the S_aO_2 from a pulsatile oximetry measurement. In both, the calibration curve must be able to adapt to the background optics of the medium. This application calls this requirement "adaptive calibration."

Specifically, the calibration curve varies with changes in the optical properties

(which determine an amount of light transport) through the tissue. For example, when the tissue's blood content or blood oxygen saturation level change, the absorption coefficient of the tissue also changes. Hence the light transport changes and the calibration also needs to be changed. In particular, fetal oximeters are more sensitive to such calibration

5   problems than adult oximeters because fetal blood oxygen saturation levels can drop to much lower values than normal adult blood oxygen saturation. The calibration curve is more variable at lower blood oxygen saturation levels. The fetal oximeter, therefore, in particular, demands the proper choice of a calibration curve for each blood oxygen saturation level.

10   This invention employs findings regarding the influence of tissue optical properties and light transport on the calibration curve to provide an appropriate calibration curve in numerous physiological conditions. According to this invention, an adaptive calibration scheme is provided for selecting the proper calibration curve to interpret R to yield S_aO_2. The following definitions apply throughout this application:

15
DC_{red} = steady-state transmitted signal at red wavelength (<800 nm)
$DC_{infrared}$ = steady-state transmitted signal at infrared wavelength (>800 nm)
f_v = volume fraction of blood in tissue
S_mO_2 = oxygen saturation due to mixture of arterial and venous blood
R   = factor based on pulsatile red and infrared signals

20   S_aO_2 = oxygen saturation of arterial blood

According to one embodiment of this invention, a method for adaptively-calibrating a pulsed oximeter is provided, which uses the steady-state or DC component of light transmission measurements to select an appropriate calibration curve. The

25   selected calibration curve is then used to properly interpret the pulsatile factor (or "R value") obtained from a standard measurement of the pulsatile components to yield an accurate arterial blood oxygen saturation (S_aO_2) measurement.

FIG. 1 is a schematic flow diagram illustrating a method of determining an arterial blood oxygen saturation (S_aO_2) level according to one embodiment of this invention.

30   FIG. 1A is a system level view of an oximetry system for implementing the method of FIG. 1. Referring to FIG. 1, a method for determining the arterial blood oxygen saturation level, according to this embodiment, begins with a one-time calibration

experiment 10. These experiments compare the DC component of light transmission measurements for both red and infrared wavelengths in air (or some other standard medium) with similar light transmission measurements taken when the probe is placed in contact with the desired tissue. In other words, two calibration measurements, one at

5   each wavelength, are taken in air and compared with two calibration measurements, one at each wavelength, taken in the tissue. The two measurements in air are initial, one-time measurements that allow correction for variation in the power of the light source (e.g., light emitting diodes or laser diodes) and variation in the responsivity of the light detector (e.g., light transducer or photodiode). Subsequent measurements of the tissue (e.g., skin)

10   are normalized using the air measurements.

A calibration factor G is also determined for each of the light wavelengths during the initial calibration process 10. The calibration factors are used to convert the ratio (M_{skin}/M_{air}) between subsequent light transmission measurements 20 of the probe in tissue (M_{skin}) and the previous air measurements (M_{air}) into a light transport factor, T, for each

15   of the light wavelengths according to the following equations:

$$T_{ir} = G_{ir} \frac{M_{ir.skin}}{M_{ir.air}}$$

$$T_{red} = G_{red} \frac{M_{red.skin}}{M_{red.air}}$$

The red and infrared light transport factors (T_{red} and T_{ir}, respectively) are in turn used to specify two unknowns, namely, the volume fraction of blood in the tissue (f_v) and the mixed blood oxygen saturation for the combined arterial and venous vasculature (S_mO_2)

20   using a grid mapping 30.

Alternatively, however, the ratios of measurements in tissue to measurements in air (M_{skin}/M_{air}) can be directly mapped by a grid mapping 30 into values for the blood volume fraction and the mixed blood oxygen saturation, bypassing the need for calibration factors G_{red} and G_{ir} and transport factors T_{red}, T_{ir} incorporating the calibration

25   factors. Also, as mentioned previously, the measurements of air at red and infrared wavelengths can be substituted by measurements of some other standard material at those

wavelengths. The ratios of the measurements of tissue to the measurements of the other standard material at red and infrared wavelengths is used to correct for source and photodector variations.

The grid mapping 30 is the result of calculations based on optical transport theory.

5   In particular, optical transport theory is used to create a unique one-to-one mapping of T_{red}, T_{ir} (or $M_{red.skin}/M_{red.air}$, $M_{ir.skin}/M_{ir.air}$) into f_v, S_mO_2. Once the blood volume fraction f_v and mixed blood oxygen saturation S_mO_2 values have been obtained, the S_mO_2 value is used to select a set of calibration curves 40 relating R to S_aO_2 from among a plurality of sets calibration curves 50. The blood volume fraction f_v is then used to select an

10   appropriate calibration curve 42 from the selected set of calibration curves 40. Optical . transport theory is also used to generate each of the calibration curves.

Once the appropriate calibration curve 42 has been selected, the pulsatile factor R can be properly interpreted to yield an accurate arterial blood oxygen saturation value S_aO_2. As a main benefit of this method, if the blood volume fraction f_v or mixed blood

15   oxygen saturation S_mO_2 of the patient's tissue site changes, the calibration will correspondingly change to allow the continued accurate determination of S_aO_2 values. As stated above, the ability of this method to readily adapt to changes in the tissue by continuously reselecting an appropriate calibration curve is called adaptive calibration. Adaptive calibration offers significant advantages over the prior art because it offers

20   accuracy over a much wider range of blood oxygen saturation levels.

The optical properties of the tissue affect the transmission of light through the tissue. Interpretation of pulsatile signals and the choice of the appropriate calibration curve therefore also depend on the baseline optical properties of the tissue. To choose the appropriate calibration curve, therefore, the optical properties of the tissue must first be

25   characterized. Important to this invention, it has been discovered that the non-pulsatile (steady-state or DC) measurements of transmitted light can be used to accomplish this task. As the tissue's blood content or blood oxygen saturation changes, the DC measurements (DC_{red}, $DC_{infrared}$) will also change, and the choice of calibration curve can be changed to provide accurate S_aO_2 approximations.

Fortunately, once recognized, the principles according to this invention are fairly straightforward to implement into an oximetry system that is similar in many respects to a conventional oximetry system. For instance, the basic circuitry and software for obtaining a pulsatile factor R with an optimal signal-to-noise can be retained.

5   Additionally, the DC signals needed to calibrate the system are already measured in conventional systems and used to calculate the pulsatile R, although they are otherwise generally disregarded. The improved oximetry system according to this invention, therefore, need only be modified to permit adaptive calibration of the system. In other words, the data obtained from the current oximetry systems needs to be analyzed by an

10   additional software module (or hardwired circuitry) to determine the appropriate calibration curve for interpretation of R to yield a predicted S_aO_2. This invention provides an algorithm for selecting the proper calibration curve based on the measured DC signals.

Referring to FIG. 1A, an oximetry system according to an embodiment of this

15   invention includes an oximeter 100 configured to communicate with a data processor, such as a computer 120, through an analog to digital (A/D) converter 110. A display device, such as a monitor 130, can also be provided for viewing a visual representation of the physiological characteristics of a patient. According to this embodiment, the oximeter 100 includes a light source and a light transducer. The light source is capable of

20   providing light of a first wavelength and a second wavelength (preferably red and infrared) to a patient's tissue (i.e., finger, ear lobe, fetal scalp skin, etc.). The light transducer communicates data regarding the transmission of light through (or reflection of light from) the tissue to the data processor 120 through the A/D converter 110. The data processor uses the light transmission data to determine an arterial blood oxygen saturation

25   S_aO_2 level of the tissue using software adapted to cause the computer 120 to implement the method described herein. The software can be provided to the computer 120 on a computer readable medium such as a floppy disk, a CD ROM, etc., or via any other type of data transfer mechanism. A display device 130 is used to convey information regarding the S_aO_2 level to the attending physician to facilitate appropriate treatment.

FIG. 2 is a block diagram illustrating the basic algorithm for determining arterial blood oxygen saturation levels according to one embodiment of this invention. Referring to FIG. 2, although this basic algorithm utilizes the same calculation of the pulsatile factor R, based on the AC components of the light transmission measurements, as used in the prior art, it further adds the selection of an appropriate calibration curve. As indicated, the calibration curve is chosen based on the DC components of the light transmission measurements. The basic adaptive calibration algorithm according to this embodiment begins by using the DC components of light transmission measurements $(DC_{red}, DC_{infrared})$ to yield the light transport factors T_{red}, T_{ir}. The light transport factors T_{red}, T_{ir} are then mapped into a unique blood volume fraction f_v, and a mixed blood oxygen saturation value S_mO_2. These values are representative of absorption and scattering characteristics of the tissue and can be used to adaptively select an appropriate R vs. S_aO_2 calibration curve.

An enlarged view of the grid mapping 30 of FIG. 1 is shown in FIG. 3. As noted above, the probe photodiode measurements on skin at both red and infrared light wavelengths $M_{red\,skin}, M_{ir\,skin}$ are normalized by dividing those measurements with the air calibration measurements $M_{red\,air}, M_{ir\,air}$. The normalized values $(M_{red\,skin}/M_{red\,air})$, $(M_{ir\,skin}/M_{ir\,air})$ are then multiplied by their respective calibration factor G_{red}, G_{ir} to yield a red and an infrared light transport factor T_{red}, T_{ir}, respectively. These light transport factors T_{red}, T_{ir} correspond directly to the steady-state components of the transmitted signals $DC_{red}, DC_{infrared}$ of FIG. 2.

Referring specifically to FIG. 3, the light transport factors T_{red}, T_{ir} have a well-defined meaning in optical transport theory that depend on the blood volume fraction f_v and mixed blood oxygen value S_mO_2 of the tissue. This relationship is represented by the grid mapping 30 of FIG 3. As indicated by the grid mapping 30, a light transport factor pair T_{red}, T_{ir} specifies a unique blood volume fraction and mixed blood oxygen value pair f_v, S_mO_2.

Once the f_v, S_mO_2 pair has been determined, the S_mO_2 value is used to select a specific set of calibration curves from among a plurality of sets of calibration curves,

where each set of calibration curves includes a plurality of R vs. S_aO_2 calibration curves. Each calibration curve is for a given f_v value. Accordingly, the f_v value can then be used to select an appropriate one of the calibration curves, for the given light transmission properties of the tissue, from the set of calibration curves. The selected calibration curve

5   allows the use of the pulsatile factor R to determine the arterial blood oxygen saturation level S_aO_2. Alternatively, however, the values of f_v and S_mO_2 can jointly and directly select the appropriate calibration curve R versus S_aO_2 by means of an algorithm or lookup table.

A computational model is needed for predicting how the measured pulsatile ratio

10   R will vary for changes in tissue blood content that affect absorption and for changes in tissue scattering properties. Absorption and scattering are the two optical properties that determine light transport properties. The following section provides a simple computational model for creating a calibration curve.

The optical properties of tissue are based on the absorption properties of water,

15   bloodless tissue, oxygenated whole blood, and deoxygenated whole blood, and on the scattering properties of skin tissue and blood. These are summarized as follows:

$$\mu_{a\ bloodless\ tissue} = 0.75\ \mu_{a\ water} + \mu_{a\ dry\ tissue\ absorption}$$
$$\mu_{a\ oxy\ whole\ blood} = (2.303)\ \epsilon_{oxy\ Hb}\ (150\ g/liter)/(66,500\ g\ Hb/mole) = 0.0052\ \epsilon_{oxy\ Hb}$$

20   $$\mu_{a\ deoxy\ whole\ blood} = 0.0052\ \epsilon_{deoxy\ Hb}$$

where

$\mu_{a\ water}$ = spectrum (from Hale and Querry 1973)
$\mu_{a\ dry\ tissue\ absorption} \approx 85.3exp(-(nm - 154)/66.2)\ [cm^{\wedge}-1]$ (based on in vitro

25   neonatal skin data by Saidi 1992)
$\epsilon_{oxy\ Hb}$ = Hb molar extinction coefficient spectrum (from Prahl 1998)
$\epsilon_{deoxy\ Hb}$ = Hb molar extinction coefficient spectrum (from Prahl 1998)

Some or all of the following references were helpful in obtaining the foregoing

30   approximations:

G.M. Hall, M.R. Querry, "Optical constants of water in the 200 nm to 200 μm wavelength region," Appl. Opt., 12, 555-563 (1973). See the water spectrum on website http://omlc.ogi.edu/spectra/water/index.html.

35

S.A. Prahl 1998: http://omlc.ogi.edu/spectra/hemoglobin/index.html

I.S. Saidi 1992: "Transcutaneous optical measurement of hyperbilirubinemia in neonates," PhD Thesis, Rice University. Also, see the summary of skin optics on website

5   http://omlc.ogi.edu/news/jan98/skinoptics.html. The constant offset 0.244 cm^{-1} in Saidi's approximation has been removed since this is probably due to residual hemoglobin staining in the in vitro tissue samples measured.

It should be noted that the spectrum for μ_a dry tissue absorption is a crude approxi-

10   mation only. The above μ_a dry tissue absorption is consistent with the literature data

for various reports on not quite bloodless aorta tissue samples (see for example

http://omlc.ogi.edu/spectra/aorta/index.html). There appears to be a small amount of

inevitable hemoglobin staining that dominates the absorption of in vitro tissues in the red-

infrared spectral range of interest here. Although the above spectrum approximation is

15   inaccurate at shorter wavelengths, this does not prevent its usefulness in the red-infrared

range of interest in the primary embodiments of this invention.

The scattering properties of bloodless skin tissue and whole blood are very

similar, at least with respect to their respective reduced scattering coefficients μ_s', which

determines light diffusion. The net scattering of skin is calculated as follows:

20                $\mu_s' = f_v \mu_s'\text{blood} + (1 - f_v)\mu_s'\text{bloodless skin}$

where

μ_s'bloodless skin = spectrum from Saidi et al. 1995
μ_s'blood = spectrum from Roggan et al. 1999

25   One or more of the following references were helpful in obtaining the foregoing equation:

I.S. Saidi, S.L. Jacques, F.K. Tittel, "mie and Rayleigh modeling of visible light scattering neonatal skin," Applied Optics 34:7410-7418, 1995. Also see Jacques 1998: http://omlc.ogi.edu/

30   A. Roggan, M. Friebel, Klaus Doerschel, A. Hahn, G. Mueller, "Optical properties of circulating human blood in the wavelength range 400-2500 nm," J Biomedical Optica 4:36-46, 1999. Data for μ_s and g versus wavelength for 5% hematocrit blood. These data were used to calculate μ_s' for this report, as recorded in file "blood_scatterin.m".

35

A summary of the optical properties at the two wavelengths, 730 nm and 940 nm,

used by the oximeter is given below in units of $[cm^{-1}]$:

18

Tissue	μ_a730	μ_a940	$\mu_s'730$	$\mu_s'940$
oxy blood	2.0280	6.3128	30.2715	23.5881
deoxy blood	5.7314	3.6059	30.2815	23.5881
bloodless	0.0276	0.2210	10.1402	6.9397

5

where bloodless skin properties were based on:

	μ_a730	μ_a940
water	0.0179	0.2939
dry dermis	0.0142	0.0006

10

The computational module for calculating the R vs. S_aO_2 calibration curve will now be discussed. In developing this computational model, the parameters that can be varied by the user include:

The blood volume fraction, f_v,	Describes the volume of blood per volume of tissue, a dimensionless fraction.
The arterial oxygen saturation, S_aO_2	Describes the oxygen saturation of the arterial blood supply, a value from 0 to 1 (or 0 to 100%).
The mixed blood oxygen saturation, S_mO_2	Describes the oxygen saturation of the combined venous and arterial blood supply, a value for 0 to S_aO_2 since $S_mO_2 \le S_aO_2$.

15   The following description provides two alternative algorithmic implementations of the invention written in the MATLAB™ programming language. In a first embodiment, which follows the method illustrated in FIGS. 1, 2, and 3, a program called "calibrate.m" is used to generate the calibration curves for various f_v, S_aO_2, and S_mO_2 choices. A listing of the calibrate.m program is provided as FIG. 5. The program calls a

20   subroutine called "calcR.m" which calculates the pulsatile factor R based on the equation:

$$R = calcR(optprops)$$

Where "optprops" is a vector containing the μ_s' of perfused skin, the μ_a of the mixed venous and arterial blood supply, and the μ_a of the arterial supply.

25   optprops = [musp, mua_mixed, mua_arterial]

The program "calibrate.m" begins by calling a subroutine called "tissueoptics.m" which loads the needed optical properties for all wavelengths from 250 to 1000 nm, then selects only the values for 730 and 940 nm. The optical properties are called oxy, deoxy,

skin, musp_skin, and musp_bl, for the μ_a values of oxygenated blood, deoxygenated blood, and bloodless skin, and for the $\mu_s{}'$ values of bloodless skin and whole blood, respectively. For example, oxy(1) and oxy(2) are the μ_a oxy at 730 nm and 940 nm, respectively. All blood values are for 45% Hct blood.

The calibrate.m program then sequentially chooses a value for f_v from 0.01 to 0.20:

```
for i = 1:20
    fv = I*0.01; % choose series of blood volume fractions
```

And for each f_v chooses a series of S_aO_2 values from 0 to 1.00 (0-100%):

```
for j = 1:51
    SaO2 = (j-1) / 50; % choose series of SaO2 values
```

The S_mO_2 value is automatically chosen to be some fraction of the S_aO_2, for example:

```
SmO2 = SaO2*0.80; % choose SmO2 = fraction of SaO2
```

In the above case, the fraction was chosen to be 0.80 or 80% of the S_aO_2. Any fraction $0 \leq f \leq 1$ can be chosen. Physically, S_mO_2 cannot exceed S_aO_2.

Once the choices of f_v, S_aO_2, and S_mO_2 are made, the program proceeds to calculate the optical properties of the tissue:

```
mua_arterial = SaO2 * oxy + (1-SaO2) *deoxy;
mua_mixed = fv* (SmO2 * oxy + (1-SmO2) *deoxy) + (1 - fv) *skin;
musp = fv*musp_bl + (1-fv) *musp_skin;
```

Which are the absorption of the arterial blood supply, the absorption of the mixed venous and arterial blood supply, and the scattering of the tissue, respectively. These properties are assigned to the vector optprops.

Finally, the program calls the subroutine calcR.m:

```
R(j) = calcR(optprops);
```

The R value returned is assigned to the array element R(j) to facilitate later plotting. The S_aO_2 value is assigned to the array element SO2(j) for later plotting. After calculating R(j) and SO2(j) for all the S_aO_2 values, the curve is plotted. The next volume fraction f_v is then computed and the process repeats. Accordingly, each calibration curve is for a

separate f_v.

A listing of the calcR.m subroutine is provided in FIG. 6. The calcR.m subroutine will now be described in detail. The function assumes that the "effective source-detector distance" is d = 0.55 cm, as was deduced from the diffusion theory analysis of the

5   phantom experiments. The transport factor T $[cm^{-2}]$ is calculated for the red and infrared wavelengths, i.e., for j=1:2. If a source power S [W] was specified, then the product S*T would equal the fluence F $[W/cm^2]$ at the detector.

First, the absorption coefficient mua is assigned the value based on the mua_mixed value, which describes the blood content prior to a heart beat. The optical

10   diffusion length D and the optical penetration depth delta are calculated. The transport factor T1 is calculated according to the equation:

$$T1(j) = exp (-d/delta) / (4*pi*D*d)$$

Next, a very small perturbation in the absorption coefficient mua is achieved by adding a

15   small fraction (0.001) of the mua_arterial:

$$mua = mua\_mixed(j) + 0.001*mua\_arterial(j)$$

Then the transport factor T2 is calculated:

$$T2(j) = exp (-d/delta) / (4*pi*D*d)$$

20

Finally, the pulsatile factor R is calculated in the standard fashion. Specifically, the "difference/mean" factors of the measurements before and after added arterial blood are determined, and the red/infrared ratio of these factors is then calculated according to the following equations:

25   A_730 = (T2(1) - T1(1))*2/(T2(1) + T1(1)); % RED;
          A_940 = (T2(2) - T1(2))*2/(T2(2) + T1(2)); % INFRARED;
          R = A_730/A_940

This R value is then returned to the calibrate.m program.

30   Using the R values, the program calibrate.m generates the R vs. S_aO_2 calibration curves for various values of f_v. FIG. 4 shows a set of calibration curves 40 for various blood volume fractions f_v = 0.01 to 0.20 at a specified S_mO_2 level. To generate these curves, the value of S_mO_2 was set at $0.80*S_aO_2$. Referring to FIG. 4, as the blood volume

21

(represented by the fraction f_v) increases, the calibration curve moves downward toward lower R values. At first, increases in blood volume have a big effect. Later, at high blood contents, small additions of blood have less effect. The curves converge on a limiting calibration curve at very high blood contents. It should be noted that diffusion theory is

5 not accurate at very high absorption coefficients, so the calibration curves at very high blood contents are not accurate. Fortunately, however, real skin perfusion does not usually range sufficiently high to violate the accuracy of diffusion theory.

It should be noted that the choice of S_mO_2 affects the calibration curves as well. The convention is followed that S_mO_2 is chosen to be a fraction $(0 \leq f \leq 1)$ of the S_aO_2

10 level. The S_mO_2 value can only be less than or equal to the arterial oxygen saturation S_aO_2. Deoxygenation causes the calibration curves to fall slightly downward.

The effect of scattering on the calibration curve will now be discussed. First, consider a water solution in which hemoglobin has been added. The solution is clear. There is no light scattering. We can mimic the pulsatile blood content by simply adding a

15 very small amount of hemoglobin to the solution. Measurements of light transmission before and after the addition constitute a "pulsatile" signal which allows a calculation of the pulsatile R value. The following programming statements replaced the diffusion theory statements in calcR.m to mimic transmission through a clear solution:

```
mua = mua_mixed (j);
T1(j) = exp (-d*mua);
mua = mua_mixed (j) + 0.001*mua_arterial (j)'
T2(j) = exp (-d*mua)
```
20

Importantly, the calibration curves for the clear solution of hemoglobin (Hb), for

25 all values of $f_v = 0.01$ to 0.20 are identical. Without scattering, the R value is insensitive to blood volume fraction f_v. Scattering is therefore very important to the calibration curve of R vs. S_aO_2. It should be noted, however, that variation in the optical properties of the skin by a factor f that ranges from 0.5 to 2.0 has a negligible effect on the calibration curve. In other words, when the skin scattering properties range from 1/2 to twice

30 normal, this 4-fold variation has negligible effect on the calibration curve, yet the curve is quite different from the clear solution of Hb. Since the scattering of neonatal skin is

variable, dependent on the gestational development of collagen fibers in the neonate, the insensitivity of the pulsatile R value to variations in scattering in very important. As long as there is sufficient scattering to cause light to diffuse from source to detector, the calibration curve is otherwise insensitive to variations is $\mu_s{'}$.

5   Animal studies monitored the R measurements on skin with the spiral oximeter probe while measuring the S_aO_2 directly with an intravascular catheter probe. According to this research, the major determinant of the calibration curve is the blood volume fraction, f_v. The highest curve was obtained for a sheep which might have had a blood volume of 3%. The other animals showed values in the 6-8% range. The lowest curve

10   for one pig, however, is below even the 20% blood volume fraction level. This demonstrates that another factor besides f_v affects the calibration curve. That factor is mixed blood oxygen saturation S_mO_2.

As was discussed before, lowering the selected S_mO_2 value moves the calibration curves downward. The lowest pig curve from the animal experiments probably

15   corresponds to a situation in which the S_mO_2 was low. In summary, the basic behavior of the animal data is mimicked by the calibrate.m program. A method of guessing what the choices of f_v and S_mO_2 should be to specify the correct calibration curve will be addressed next.

As in the prior art, the two signals from the detector obtained during sequential

20   illumination by the red LED and by the infrared LED are analyzed by special circuitry and software to determine the pulsatile factor R with a good signal-to-noise ratio. The raw signals also, however, have an average DC value that is related to the two parameters of interest, f_v and S_mO_2. Referring back to FIG. 1, the basic steps of adaptive calibration according to one embodiment of this invention, include: (1) air calibration; (2) using the

25   "grid.m" software program to allow T_{ir}, T_{red} to uniquely specify f_v, S_mO_2; (3) using S_mO_2 to select a set of calibration curves; and (4) using f_v to select a single calibration curve. These steps will now be described in further detail.

As shown in FIG. 1, two measurements, one each at the red and infrared wavelengths, are made first with the probe in air again when the probe is attached to the

fetal scalp skin. Hence, four measurements are obtained: $M_{red\ air}$, $M_{ir\ air}$, $M_{red\ skin}$, $M_{ir\ skin}$. The ratio $M_{red\ skin}/M_{red\ air}$ is equivalent to:

$$\frac{M_{redskin}}{M_{redair}} = \frac{Sg1T_{redskin}Ag2D}{Sg3T_{redair}Ag4D} = \frac{g1g2}{g3g4T_{redair}}T_{redskin}$$

Where:

g1 = factor describing how the power of the source is augmented by reflections from the mirrored surfaces of the spiral probe when in skin,

g2 = Factor describing how transmitted power couples to the detector through the tissue/epoxy/photodiode interfaces,

g3 = Factor describing how the power of the source is augmented by reflections from the mirrored surfaces of the spiral probe when in air,

g4 = Factor describing how transmitted power couples to the detector through the air/epoxy/photodiode interfaces,

S = Power of the LED source [W],

A = Area of collection at the detector [cm2],

D = Detector responsivity [volts/W]

5   The normalization step (i.e., calculating a ratio between the light transmission measurements) cancels the influence of the factors S, A, and D. Hence, the effect of variations in the LED power or the photodetector responsibility are removed from the measurement. The above equation can alternatively be arranged:

$$R_{redskkin} = \frac{M_{redskin}}{M_{redair}}\frac{g_3g_4T_{redair}}{g_1g_2} = \frac{M_{redskin}}{M_{redair}}G_{red}$$

10   Where G_{red} equals $T_{red\ air}\,g3g4/g1g2$. A similar expression yields $T_{ir\ skin}$ using G_{ir}.

The values of the factors G_{red} and G_{ir} must be experimentally determined. Such an experiment involves measuring M_{air} for the red and infrared wavelengths. Once the air measurements are made, the probe is then inserted in a phantom tissue solution of known

15   optical properties. In this manner, the value of the light transport factor T [cm^{-2}] can be calculated for the respective optical properties at the red (730 nm) and infrared (940 nm) wavelengths using the equation:

$$T = \frac{\exp(-d\sqrt{\mu_a/D})}{4\pi Dd}$$

Where

μ_a = absorption coefficient [cm^{-1}],
D = diffusion length [cm] = $1/(3(\mu_a+\mu_s'))$,
μ_s' = reduced scattering coefficient [cm^{-1}],
d = the effective source-detector distance [cm].

For this embodiment, the experimental testing involved the testing of 24 spiral oximeter probes by taking a measurement in air followed by a measurement in 2% intralipid, for both the red and infrared wavelengths (i.e., 4 measurements). The value of light transport factors T for the red and infrared wavelengths were calculated based on the optical properties of the phantom. The values G_{red} and G_{ir} were then calculated using the expressions:

$$G_{red} = \frac{T_{red}}{(M_{redIL} / M_{redair})}$$

$$G_{ir} = \frac{T_{ir}}{(M_{irIL} / M_{irair})}$$

FIG. 7 shows the values of G_{red} and G_{ir} that were obtained using the above experiment. The analysis was accomplished using the MATLAB program "calcG.m," the listing for which is shown in FIG. 8. Ignoring probe #2, the mean values for G were 1.036 ± 0.031 for red and infrared, respectively.

A program called "grid.m," a listing of which is shown in FIG. 9, is used to generate the grid that describes the relationship between f_v and S_mO_2 and the values T_{red} and T_{ir}. The program grid.m calls a subroutine function called "calcDC.m," listed in FIG. 9A, to begin the operation. The program grid.m assumes a background scattering value μ_s' and uses the two parameters S_mO_2 and f_v to specify the two optical properties μ_a and D which are used to calculate the transport factors T_{red}, T_{ir}. A series of values are used; i.e., $f_v = 0:0.01:0.20$ and $S_mO_2 = 0:0.1:1.0$, to generate a set of T_{red} and T_{ir} values to yield the grid shown in FIG. 3. Referring to FIG. 3, the grid shows that as f_v increases, both the T_{red} and T_{ir} drop to lower values. The grid also shows that as S_mO_2 increases, the T_{red} increases while the T_{ir} decreases. Measurements of T_{red} and T_{ir} uniquely map to an f_v, S_mO_2 pair. The f_v, S_mO_2 pair, in turn, will specify a unique R vs. S_aO_2 calibration curve.

Accordingly, the f_v and S_mO_2 specify the absorption (μ_a) and scattering (μ_s') properties of the tissue, as developed by the calibrate.m program, allowing the selection of the appropriate calibration curve. The selected calibration curve is then used to match the calculated pulsatile R value from the conventional oximetry system with the S_aO_2 level.

5   Although the above description explains one approach and algorithm for accomplishing the objects of this invention, it should be noted that many different approaches and algorithms are within the contemplation of this invention. An alternative and preferred algorithm will now be described. According to a presently preferred algorithm, the time-averaged DC measurements of a standard calibration material, such as

10   air, water, or some other standard medium, ($M_{std.red}$, $M_{std.ir}$) and the DC measurements of tissue ($M_{tissue.red}$, $M_{tissue.ir}$), are derived from an oximeter to yield normalized light measurement values:

$$mT_{red} = M_{tissue.red}/M_{std.red}$$

$$mT_{ir} = M_{tissue.ir}/M_{std.ir}$$

15
Also, a pulsatile factor (R value) is obtained from the pulsatile AC component of the oximeter measurements and is called mR. These three values mT_{red}, mT_{ir}, and mR are determined and passed to a subroutine getSaO2([mTred, mTir, mR]) to yield a prediction of the arterial oxygen saturation S_aO_2 which is accurate despite variations in the blood

20   volume fraction, f_v, or the mixed blood oxygen saturation, S_mO_2. The program getSaO2(), written in the MATLAB™ programming language, is listed here:

```
        function SaO2 = getSaO2([mTred, mTir, mR])
        %%%
        % Returns the arterial oxygen saturation SaO2
25      % given the normalized measurements:
        %       mTred = M_tissue_red/M_std_red
        %       mTir  = M_tissue_ir/M_std_ir
        %%%
        [fv, SmO2] = grid(mTred, mTir)%
30      [C0 C1 C2] = calibcurve([fv, SmO2])%
        SaO2       = C0 + C1*mR + C2*mR^2;      % FINAL ANSWER
```

The function getSaO2() uses the normalized light measurement data [mTred, mTir] to specify the blood volume fraction and mixed blood oxygen saturation values [fv, SmO2],

35   which in turn specify a calibration curve for S_aO_2 as a function of R that has been

26

summarized as a second-order polynomial. The polynomial is used to convert the pulsatile measurement mR into a predicted S_aO_2. The final answer is the predicted S_aO_2.

The above function getSaO2() is the complete master routine which handles the direct feed of measurement data from an oximeter via a master program. The details of

5   the functions grid() and calibcurve() are presented in the following paragraphs. Both grid() and calibcurve() use two transport functions mTred() and mTir(). First, a description of how mTred() and mTir() are prepared is provided.

In a one-time set of calibration experiments using a particular oximeter probe design, such as a probe designed for the adult finger or a probe designed for the skin of

10   the fetal head during birth, two light transport factors $T_{red}(\mu_a, \mu_s')$ and $T_{ir}(\mu_a, \mu_s')$ are specified by measurements in a series of calibrated phantoms of known optical properties consisting of various absorption coefficients (μ_a) and reduced scattering coefficients (μ_s'). at the red and infrared wavelengths. These transport factors are similar to the transport factors predicted by optical diffusion theory or other transport theories found in the

15   scientific literature but further include the influence of the specific probe geometry. They are computed from the measured values of the phantoms:

$$T_{red}(\mu_a, \mu_s') = M_{phantom.red}(\mu_a, \mu_s')/M_{std.red}(\mu_a, \mu_s')$$

$$T_{ir}(\mu_a, \mu_s') = M_{phantom.ir}(\mu_a, \mu_s')/M_{std.ir}(\mu_a, \mu_s').$$

20

These calibration experiment results are summarized by two functions, Tred(mua, musp) and Tir(mua, musp), where mua = μ_a and musp = μ_s', which receive the arguments (μ_a, μ_s') and return the expected values of ($M_{phantom.red}/M_{std.red}$) and ($M_{phantom.ir}/M_{std.ir}$). For example, implementations of Tred() and Tir() for a particular type of oximeter probe

25   using water as the standard material are shown below as two MATLAB™ programs:

```
function mTred = Tred(mua, musp)
% Returns mTred = M_red/M_std_red
% given tissue absorption (mua) and scattering (musp)
% In this case, the standard was water.
m1 = 0.7443;
m2 = 2.5435;
m3 = 0.2612;
m4 = 29.7706;
const = m1*exp(-musp/m2) + m3*exp(-musp/m4);
```

```
d       = 0.2904; % [cm] apparent source-detector distance
a       = 0.4779; % [cm^-1] an apparent background mua
D       = 1/3./((a + mua) + musp);
mueff   = sqrt((a + mua)./D);
mTred = const*exp(-mueff*d)./(4*pi*D*d);  % FINAL ANSWER


function mTir = Tir(mua, musp)
% Returns mTir = M_ir/M_std_ir
% given tissue absorption (mua) and scattering (musp)
% In this case, the standard was water.
m1 = 0.6664;
m2 = 2.5695;
m3 = 0.4168;
m4 = 27.6357;
const = m1*exp(-musp/m2) + m3*exp(-musp/m4);
d       = 0.2825; % [cm] apparent source-detector distance
a       = 0.3143; % [cm^-1] an apparent background mua
D       = 1/3./((a + mua) + musp);
mueff   = sqrt((a + mua)./D);
mTir = const*exp(-mueff*d)./(4*pi*D*d);  % FINAL ANSWER
```

The function grid() uses Tred() and Tir() in conjunction with an optical properties library which is loaded by the command "load tissueoptics". This library includes the spectral optical absorption properties of oxy-hemoglobin in whole blood (oxy), deoxy-hemoglobin in whole blood (deoxy), and bloodless tissue (mua_tissue), and the optical scattering properties of the tissue (musp_tissue) and of blood (musp_blood). The absorption properties of bloodless tissue are based on the absorption properties of water and the non-aqueous components of bloodless tissue. This library is prepared from values in the scientific literature. For example, for skin the library is specified by values from the scientific literature as follows:

```
%%%
% Created by the command "load tissueoptics"
% In this case, tissue is skin, red = 730 nm, infrared = 900 nm
%%%
oxy         = [2.03, 6.31];      % [mua_red, mua_ir], as [cm^-1]
deoxy       = [5.73, 3.61];      % [mua_red, mua_ir]
mua_tissue  = [0.0276, 0.221];   % [mua_red, mua_ir]
musp_tissue = [10.2, 6.94];      % [musp_red, musp_ir]
musp_blood  = [30.3, 23.6];      % [musp_red, musp_ir]
```

The subroutine grid() uses a standard minimization algorithm, called fmins() in MATLAB™, and an error evaluation function fvSmO2grid() to directly calculate f_v and S_mO_2 based on the measurements [mTred, mTir]:

$$[fv, SmO2] = grid([mTred, mTir])$$

An implementation of the functions grid() and fvSmO2grid() are shown below in

28

MATLAB™ format:

```
%%%
% function [fv SmO2] = grid(mTred, mTir)
%         where
%             mTred = mua_red/mua_std_red
%             mTir  = mua_ir/mua_std_ir.
% Program returns the values for blood volume fraction (fv)
% and mixed blood oxygen saturation (SmO2).
% Uses the functions Tred(mua, musp) and Tir(mua,musp) functions
%  determined experimentally in phantoms of known optical
properties.
% The values mua_red and mua_ir refer to DC measurements on
tissues
% and mua_std_red and mua_std_ir refer to measurements
% of the standard.
%%%
global Data    % Links Data to the subroutine grid([fv SmO2]).
               % The array Data is described below.
load tissueoptics;  % Loads the optical properties as two numbers
each,
               % [value for red, value for ir] for the
following:
               % oxy(1:2), deoxy(1:2), musp_bl(1:2),
               % mua_tissue(1:2), and musp_tissue(1:2)
               % which are defined below:
Data = zeros(6,2);  % Establish size of array.
Data(1,1:2) = [mTred, mTir]; % normalized tissue measurements
Data(2,1:2) = oxy;            % mua of oxy whole blood (45%
hematocrit)
Data(3,1:2) = deoxy;          % mua of whole deoxy blood (45%
hematocrit)
Data(4,1:2) = musp_bl;     % musp of whole blood (45% hematocrit)
Data(5,1:2) = mua_tissue;  % mua of bloodless tissue
Data(6,1:2) = musp_tissue; % musp of bloodless tissue

% Call the minimization subroutine, fmins(), that finds [fv SmO2]
% based on [mTred mTir].
% An initial guess is provided to fmins() which then iteratively
% uses fvSmO2grid([fv SmO2]) to determine the error in the current
% choice of [fv SmO2] then improves its choice of [fv SmO2].
% When the error is minimized, then [fv SmO2] is returned.
fv = 0.10;    % an initial guess
SmO2 = 0.70;  % an initial guess
Start = [fv SmO2];
[fv SmO2] = fmins('fvSmO2grid', start);  % FINAL ANSWER returned
```

```
        function err = fvSmO2grid(choice)
        %%%
        % This subroutine uses a choice for [fv SmO2] = choice provided
        % by the standard MATLAB minimization program called fmins()
        % to predict values of pT = M/M_std for red and infrared
        % wavelengths. These predictions are compared with the
        % actual measurements which are passed to this subroutine from
        % the program grid() via the global variable Data(1, 1:2) =
        % [mTred mTir]. The sum of the squared differences between
        % [mTred mTir] and [pTred pTir] constitutes the "error"
        % between measurement and prediction, and this error is
        % returned to the calling function fmins(). The routine fmins()
        % iteratively calls this subroutine and improves its choice
        % for [fv SmO2]. Eventually the error is minimized and fmins()
        % stops iterating and returns the best estimate for [fv SmO2] to
        % the main program.
        %%%
        global Data  % links Data from program grid() to this subroutine
        %%% Choices being checked:
            fv              = choice(1);
            SmO2            = choice(2);
        %%%  Data provided via global variable Data(6,2):
            mT              = Data(1,1:2);  % [mTred, mTir]
            oxy             = Data(2,1:2);  % mua of oxy whole blood
            deoxy           = Data(3,1:2);  % mua of deoxy whole blood
            musp_bl         = Data(4,1:2);  % musp of whole blood
            mua_tissue      = Data(5,1:2);  % mua of bloodless tissue
            musp_tissue     = Data(6,1:2);  % musp of tissue
        %%%  Linearly mix optical components to yield mua and musp:
            mua     = fv*(SmO2*oxy + (1-SmO2)*deoxy) + (1-fv)*mua_tissue;
            musp    = fv*musp_bl + (1-fv)*musp_tissue;
        %%%  Predict measurements:
            pTred   = Tred(mua(1), musp(1));
            pTir    = Tir(mua(2), musp(2));
        %%%  Sum squared differences between measurements and
        % predictions for return to fmins():
            err     = (pTred - mT(1))^2 + (pTir - mT(2))^2;  % FINAL ANSWER
```

Once the f_v and S_mO_2 of the tissue are specified, the function calibcurve() is used

to return a calibration curve for S_aO_2 versus R:

$$[C0, C1, C2] = \text{calibcurve}([fv, SmO2])$$

where S_aO_2 is represented by a second order polynomial of the form:

$$SaO2 = C0 + C1*R + C2*R^2$$

By stepping through a set of S_aO_2 values and using the f_v and S_mO_2 values, a series of μ_a

and μ_s' values for the blood perfused tissue are generated for the red and infrared

wavelengths. These values are sent to the subroutines Tred(mua, musp) and Tir(mua,

musp) to return predictions of time-averaged measurements ($M_{tissue.red}/M_{std.red}$) and

($M_{tissue.ir}/M_{std.ir}$). Then, an incremental amount of arterial blood is added to the computer-

simulated tissue by increasing the μ_a and μ_s' values as if a 0.1% increase in blood volume fraction had occurred due to the added arterial blood. Again, the subroutines Tred(mua, musp) and Tir(mua, musp) are used to return predictions of the pulsatile measurements $M_{tissue.red}/M_{std.red}$ and $M_{tissue.ir}/M_{std.ir}$ acquired at the peak in blood volume fraction due to

5   expanded arterial volume. Then the pulsatile R value is calculated according to the equation:

$$R = [(M_{tissue.red}/M_{std.red})/(M_{tissue.red}/M_{std.red})] / [(M_{tissue.ir}/M_{std.ir})/(M_{tissue.ir}/M_{std.ir})]$$

By repeating the above for each choice of S_aO_2, one generates the conventional

10   calibration curve R versus S_aO_2, which is inverted to read as S_aO_2 versus R. A second-order polynomial is fit to this inverted calibration curve such that:

$$SaO2 = C0 + C1*R + C2*R^2$$

This polynomial allows immediate evaluation of a measured pulsatile mR value from the

15   oximeter to yield an arterial oxygen saturation value S_aO_2:

$$SaO2 = C0 + C1*mR + C2*mR^2$$

This value SaO2 is the final answer of the algorithm.

The subroutine calibcurve() is listed below. The subroutine uses the subroutine

20   calcR(optprops) to compute the expected pulsatile R for a specified set of optical properties specified by the argument optprops which holds the optical properties of the tissue with mixed arterial/venous blood and of arterial blood. For each of 51 choices of SaO2, 51 values of R are generated using calcR(). Then a second-order polynomial is fitted to the relation of SaO2(1:51) versus R(1:51) to yield the coefficients [C0, C1, C2].

25

```
function  [c2 c1 c0] = calibcurve([fv SmO2])
%%%%%
% Given [fv, SmO2], this program
% returns the answer  [c2 c1 c0]
%     where  SaO2 = c0 + c1*R + c2*R^2
%     and R is the pulsatile factor from a pulsed oximeter.
% Program creates the calibration curve R versus SaO2
% then fits the program with a second-order polynomial.
% Uses  subroutine calcR() and optical properties array Data(6,2).
%%%%
global Data
% Data provided:
mT          = Data(1,:);   % NOT USED HERE
oxy         = Data(2,:);   % mua of oxy whole blood
deoxy       = Data(3,:);   % mua of deoxy whole blood
```

30

35

```
    musp_bl      = Data(4,:);  % musp of whole blood
    mua_tissue   = Data(5,:);  % mua of tissue
    musp_tissue  = Data(6,:);  % musp of tissue
    % Cycle through series of SaO2 values = 0 to 1.00
5   for j = 1:51
        SaO2(j)      = (j-1)/50;
        mua_arterial = SaO2(j)*oxy + (1-SaO2(j))*deoxy;
        mua_mixed    = fv*( SmO2*oxy + (1-SmO2)*deoxy ) + (1-
    fv)*mua_tissue;
10      musp         = fv*musp_bl + (1-fv)*musp_skin;
        optprops     = [musp, mua_mixed, mua_arterial];
        R(j)         = calcR(optprops); % Calculate pulsatile R value
    end
    [c2 c1 c0] = polyfit(R, SaO2, 2); % where SaO2 = c0 + c1*R +
15  c2*R^2
                                    % FINAL ANSWER

    function R = calcR([fv, SmO2, SaO2])
    %%%
    % calcR.m
20  % Returns pulsatile value R = calcR(optprops),
    %   where optprops = [musp_red musp_ir mua_mixed_red mua_mixed_ir
    %                     mua_arterial_red mua_arterial_ir]
    %%%
    musp         = optprops(1:2);
25  mua_mixed    = optprops(3:4);
    mua_arterial = optprops(5:6);
    %%%
    % For time-averaged blood content
    %%%
30  mua(1) = mua_mixed(1);
    mua(2) = mua_mixed(2);
    T1(1) = Tred(mua(1), musp(1)); % red
    T1(2) = Tir(mua(2), musp(2));  % infrared
    %%%
35  % For peak arterial blood content = a 0.1% increment in blood
    content
    %%%
    mua(1) = mua_mixed(1) + 0.001*mua_arterial(1);
    mua(2) = mua_mixed(2) + 0.001*mua_arterial(2);
40  T2(1) = Tred(mua(1), musp(1)); % red
    T2(2) = Tir(mua(2), musp(2));  % infrared
    %%%
    % Calculate pulsatile R value
    %%%
45  A_red= (T2(1) - T1(1))/T1(1);  % RED
    A_ir = (T2(2) - T1(2))/T1(2);  % INFRARED
    R = A_red/A_ir;   % FINAL ANSWER
```

Finally, the coefficients [C0, C1, and C2] can be used to interpret the measured pulsatile

50   factor mR received from the oximeter as described above.

Having described and illustrated the principles of the invention in various

embodiments thereof, it should be apparent that the invention can be modified in

arrangement and detail without departing from such principles. I therefore claim all

modifications and variations coming within the spirit and scope of the following claims.

CLAIMS

5 What is claimed is:

1. A method for calibrating an oximeter for use in determining an arterial blood oxygen saturation level in tissue, comprising:

determining a steady-state component of a light transmission through or reflection

10 from a tissue at each of a first and second wavelengths;

using the steady-state component of the light transmission or reflection to select a calibration curve, said calibration curve representing a level of arterial blood oxygen saturation in relation to a pulsatile factor;

determining the pulsatile factor; and

15 determining the arterial blood oxygen saturation level using the selected calibration curve and the pulsatile factor.

2. A method according to claim 1, wherein the calibration curve is chosen from a set of calibration curves, and wherein the set of calibration curves is selected from a plurality

20 of sets of calibration curves.

3. A method according to claim 1, wherein the steady-state component of the light transmissions of the first and second wavelengths are determined by comparing measured amounts of light of the first and second wavelengths passing through a standard medium

25 with measured amounts of light of the first and second wavelengths, respectively, passing through the tissue.

4. A method according to claim 1, further comprising normalizing the steady-state component of the light transmission or reflection to remove the effects of variation of a

30 strength of a light source and a sensitivity of a transducer from the steady-state component.

5.   A method according to claim 1, wherein determining the pulsatile factor is performed by measuring and comparing the AC and time averaged DC components of the light transmission through or reflected from the tissue.

5

6.   A method according to claim 1, wherein the steady-state component of the light transmissions or reflections of the first and second wavelengths are uniquely mapped to a blood volume fraction and a mixed blood oxygen saturation value.

10   7.   A method according to claim 3, wherein the comparison generates ratios of the measured amount of light in tissue to the measured amount of light in the standard medium for each wavelength, and wherein the ratios are uniquely mapped to a blood volume fraction and a mixed blood oxygen saturation value.

15   8.   A method according to claim 1, wherein the calibration curve is chosen using a mixed blood oxygen saturation value and a blood volume fraction.

9.   A method according to claim 1, further comprising repeatedly measuring an amount of light of the first and the second wavelengths passing through or reflected from

20   the tissue, and repeatedly reselecting an appropriate calibration curve based on the steady-state component of the measured amounts of light passing through the tissue or reflected from the tissue to adaptively calibrate in response to changes in a mixed oxygen saturation level and a blood volume fraction level.

25   10.   An oximetry system for measuring arterial blood oxygen saturation levels in a tissue, comprising:

a light source configured to transmit light of a first wavelength and a second wavelength to a medium;

a light transducer configured to measure an amount of the light of each of the first

and second wavelengths transmitted through or reflected from the medium and to

generate light measurement data corresponding to the measured amount of light; and

a data processor configured to use one or more steady-state components of the

light measurement data to adaptively select a calibration curve, said calibration curve

5   being representative of an amount of arterial blood oxygen saturation relative to a

pulsatile factor.

11.   An oximetry system according to claim 10, wherein the data processor is further

configured to repeatedly reselect a calibration curve based on changes in a blood volume

10   fraction level and a mixed blood oxygen saturation level.

12.   An oximetry system according to claim 10, wherein the data processor is

configured to determine the pulsatile factor based on a ratio of pulsatile components of

the light measurements normalized by the steady-state components of the light

15   measurement data, and is further configured to determine an arterial blood oxygen

saturation value using the pulsatile factor and the selected calibration curve.

13.   An oximetry system according to claim 10, wherein the data processor is

configured to normalize the light measurement data by calculating a ratio of the light

20   measurement in the tissue to a light measurement in a standard medium.

14.   An oximetry system according to claim 10, wherein the data processor is further

configured to normalize the light measurement data into normalized light measurements

and to select a calibration curve using a grid mapping, wherein the grid mapping uniquely

25   maps the normalized light measurements into a blood volume fraction and a mixed blood

oxygen saturation value, and wherein the blood volume fraction and mixed blood oxygen

saturation value can be used to select the calibration curve.

15.   A method of measuring an arterial blood oxygen saturation level in a tissue,

30   comprising:

comparing steady-state light measurements in a standard medium of light of a first and second wavelengths with steady-state light measurements in the tissue of the light of the first and second wavelengths;

measuring an amount of the light of the first and second wavelengths transmitted

5   through or reflected from the tissue to obtain a light measurement for each wavelength;

using steady-state components of the light measurements to select a calibration curve; and

using the selected calibration curve to determine an arterial blood oxygen saturation level in the tissue.

10

16.   A method according to claim 15, wherein comparing light measurements comprises normalizing the light measurements in the tissue by calculating a ratio between the light transmission measurement in the tissue and a light transmission measurement in a calibration material for light of each of the first and second wavelengths.

15

17.   A method according to claim 16, further comprising using a grid mapping to translate the normalized light measurement into a blood volume fraction and a mixed blood oxygen saturation value, wherein optical transport theory is used to create a unique mapping between the normalized light measurements and the blood volume fraction and

20   the mixed blood oxygen saturation value.

18.   A method according to claim 15, wherein using the steady-state component of the light measurements to select an appropriate calibration curve comprises:

using the steady-state component of the light measurements to determine a blood

25   volume fraction and a mixed blood oxygen saturation value;

using the mixed blood oxygen saturation value and the blood volume fraction to select the calibration curve from a plurality of sets of calibration curves.

19.   A method according to claim 15, further comprising:

36

calculating a pulsatile factor using pulsatile signals normalized by the steady-state component of the light measurements at the first and second wavelengths; and

using the pulsatile factor and the selected calibration curve to determine the arterial blood oxygen saturation level.

5

20.   A computer readable medium containing instructions adapted to cause a computer to perform the method of claim 1.

21.   A method of generating a function grid relating optical properties of a tissue to a
10   blood volume fraction and a mixed blood oxygen saturation level, comprising:

generating a light transport function for light of a first wavelength as a function of absorption and scattering coefficients and a geometry of a probe;

generating a light transport function for light of a second wavelength as a function of absorption and scattering coefficients and the geometry of the probe; and

15   using the light transport functions for light of the first and second wavelengths in conjunction with spectral optical absorption properties of blood and tissue components to generate a function grid relating measured light transmission or reflectance of a tissue to a blood volume fraction and a mixed blood oxygen saturation level.
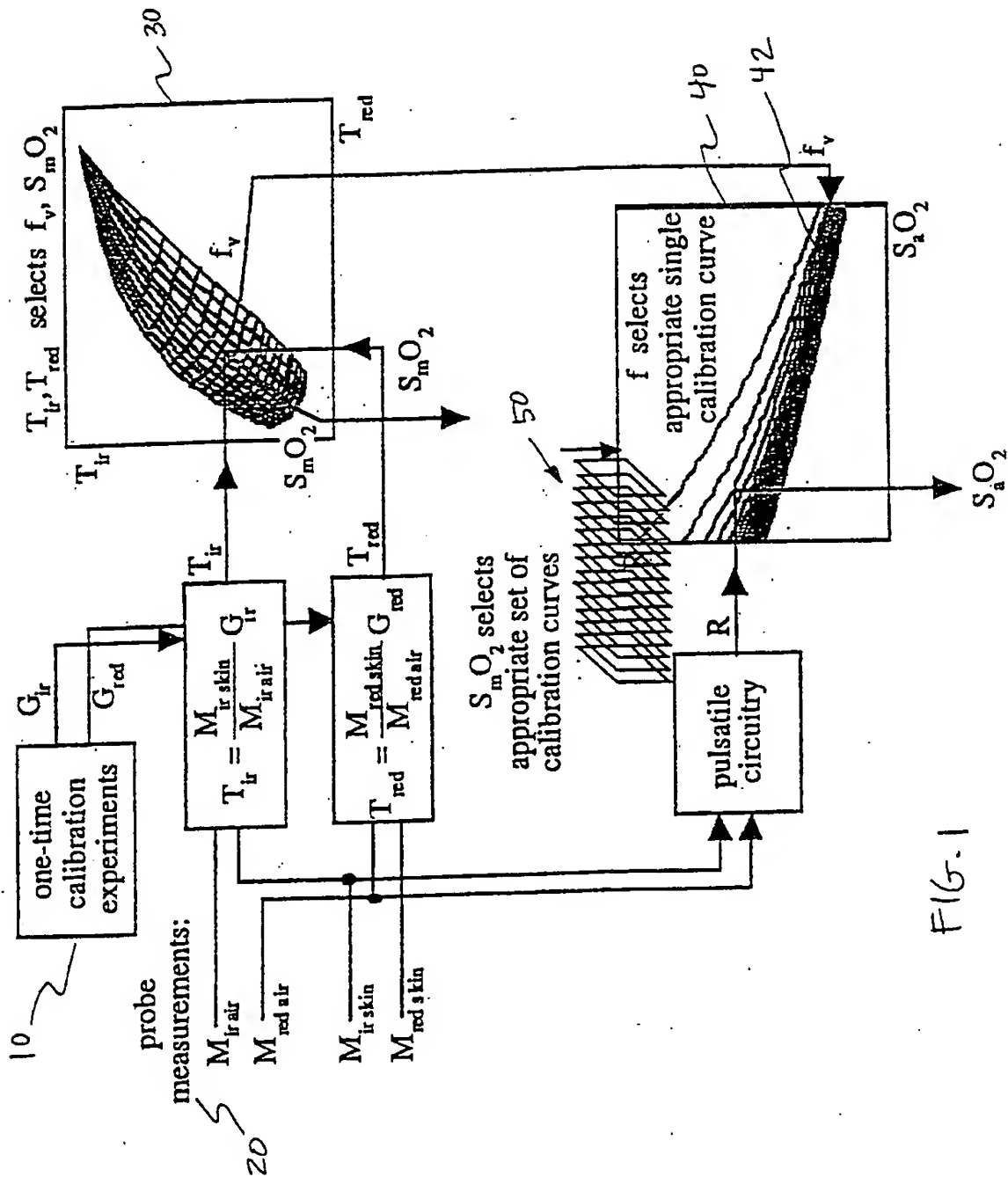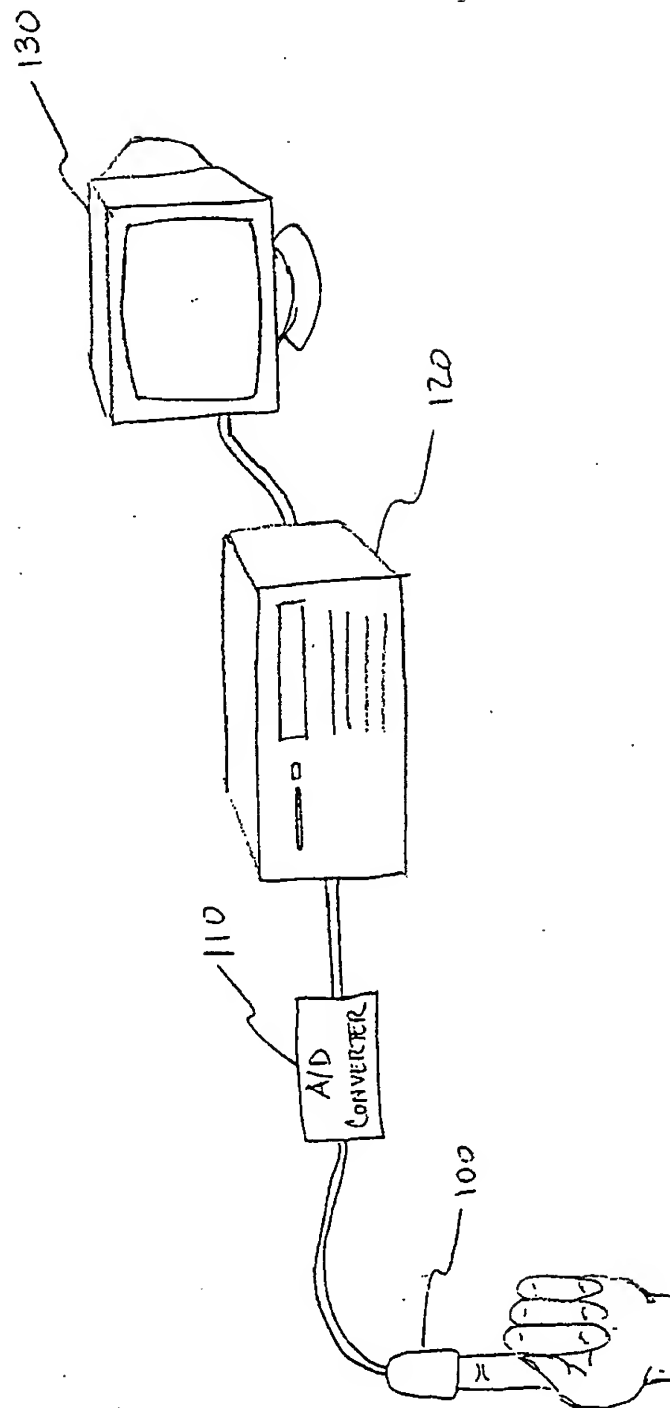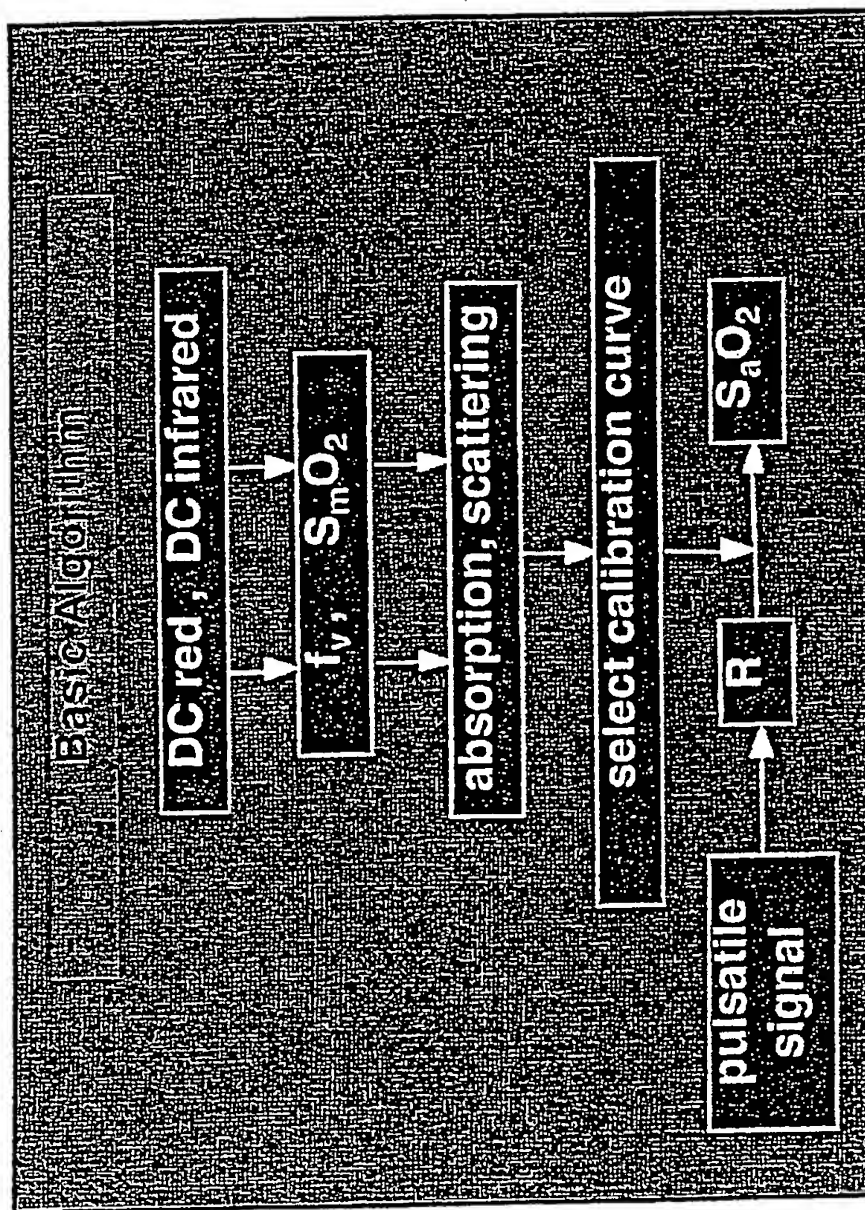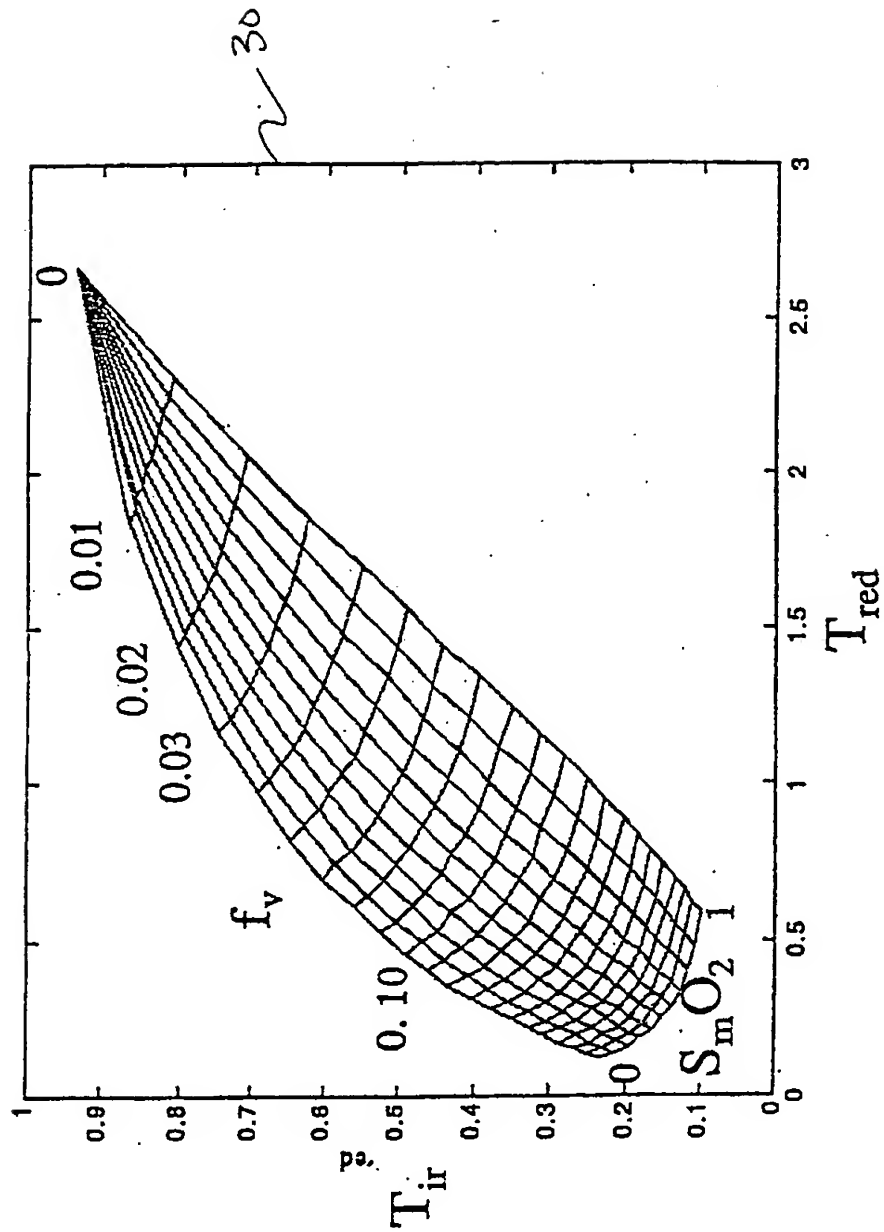
FIG. 1

FIG. IA

FIG. 2

FIG. 3

15

FIG. 4

40

CALIBRATION CURVES

fv = 0.01
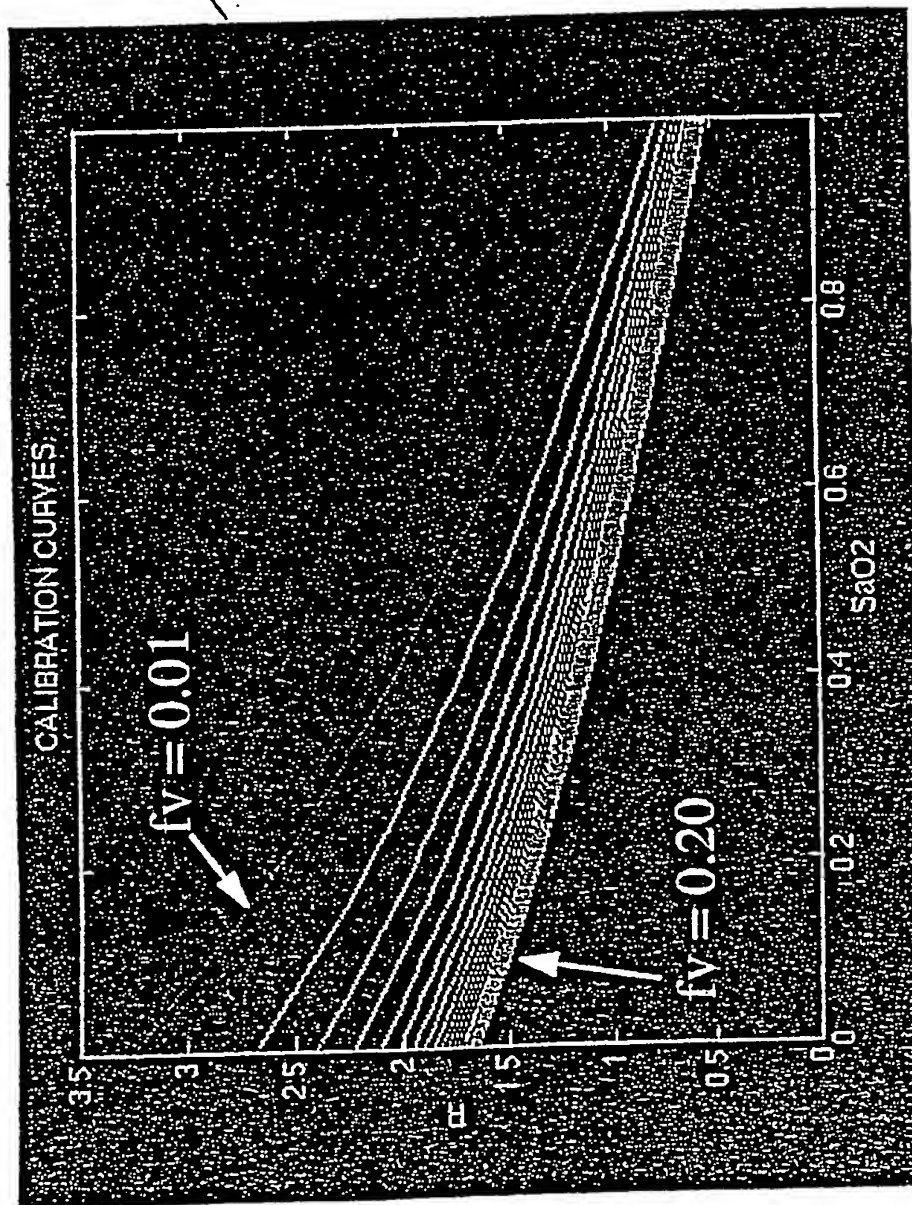
fv = 0.20

```
% calibrate.m

clear

%%%%%%
% Load nm(), oxyblood(), deoxyblood(), bloodless(),
% musp_dermis(), musp_blood()  for 250:2:1000 nm = (1:376)
% Retain only the optical properties at 730 and 940 nm.
%%%%
tissueoptics
i730 = 241;                             % index: nm(i_730) = 730
i940 = 346;                             % index: nm(i_940) = 940
oxy(1:2) = [oxyblood(i730) oxyblood(i940)];
deoxy(1:2) = [deoxyblood(i730) deoxyblood(i940)];
skin(1:2) = [bloodless(i730) bloodless(i940)];
musp_skin(1:2) = [musp_dermis(i730) musp_dermis(i940)];
musp_bl(1:2) = [musp_blood(i730) musp_blood(i940)];
clear nm oxyblood deoxyblood bloodless musp_dermis
musp_blood;

figure

for i = 1:20
      fv = i*0.01;  % choose series of blood volume fractions

      for j = 1:51
            SaO2 = (j-1)/50;   % choose series of SaO2 values
            SmO2 = SaO2*0.80;  % choose SmO2 = fraction of SaO2
                               % Note: SmO2 <= SaO2.

            mua_arterial =  SaO2*oxy + (1-SaO2)*deoxy;
            mua_mixed    = fv*( SmO2*oxy + (1-SmO2)*deoxy ) +
(1-fv)*skin;
            musp = fv*musp_bl + (1-fv)*musp_skin;
            optprops = [musp mua_mixed mua_arterial];
            R(j) = calcR(optprops);
            SO2(j) = SaO2;

      end % j
      plot(SO2, R,'y')
      hold on
      if (i==1);plot(SO2, R,'r-');end

end % i

xlabel('SaO2')
ylabel('R')
title('CALIBRATION CURVES')
axis([0 1 0 3.5])
```

FIG. 5

Page 6 of 11

```
% calcR.m

function R = calcR(optprops)

musp = optprops(1:2);
mua_mixed = optprops(3:4);
mua_arterial = optprops(5:6);

d = 0.55;

for j=1:2   % 1=red, 2=infrared

mua = mua_mixed(j);
D = 1/(mua + musp(j))/3;
delta = sqrt(D/mua);
T1(j) = exp(-d/delta)/(4*pi*D*d);

mua = mua_mixed(j) + 0.001*mua_arterial(j);
D = 1/(mua + musp(j))/3;
delta = sqrt(D/mua);
T2(j) = exp(-d/delta)/(4*pi*D*d);


end %j

%%%%%%
% Calculate R
%%%
A_730 = (T2(1) - T1(1))*2/(T2(1) + T1(1));    % RED
A_940 = (T2(2) - T1(2))*2/(T2(2) + T1(2));    % INFRARED
R = A_730/A_940;
```
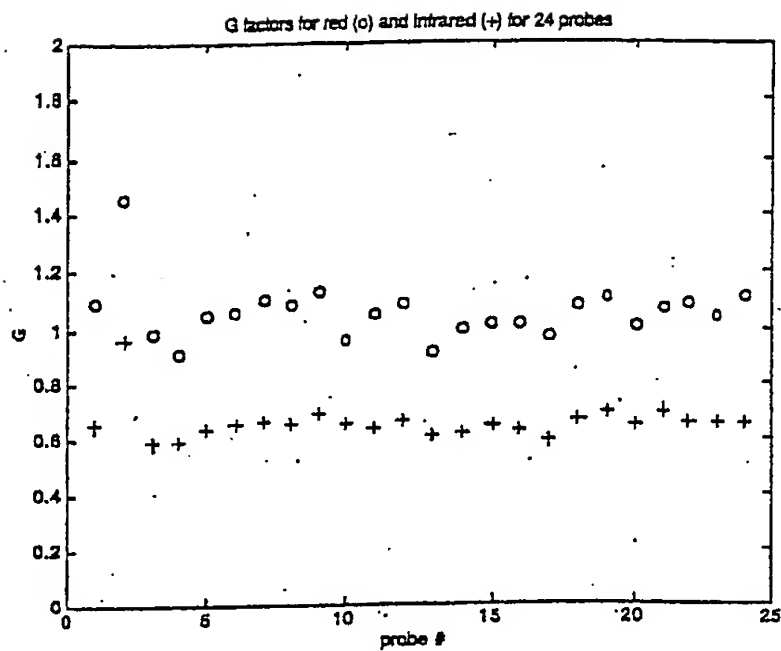
FIG. 6

G factors for red (o) and infrared (+) for 24 probes

FIG. 7

probe #

Fig. 28c The   ibration factor G for the 24 probes at the red (730 nm, circles o)
and ir (940 nm, crosses +) wavelengths, prepared by "calcG.m".

```
% calcG.m

clear
close all

%%%%%%%
% Load data from IL, air experiment
%       -->  . m(1:10, 1:4) = m(probe#, [REDil REDair IRil
IRair])
%%%%
aircalib
m(11:24,1:4) = extra(:,1:4);

d = 0.55; % cm, effective source-detector separation
figure

for i=1:24
     % red (730 nm)
     mua = 0.02;
     musp = 1.24*2;
     D = 1/3/(mua + musp);
     delta = sqrt(D/mua);
     T = exp(-d/delta)./(4*pi*D*d);
     Mil = m(i,1);
     Mair = m(i,2);
     G(i,1) = T/(Mil/Mair);
     plot(i,G(i,1),'ro')
     hold on

     % ir (940 nm)
     mua = 0.08;
     musp = 0.93*2;
     D = 1/3/(mua + musp);
     delta = sqrt(D/mua);
     T = exp(-d/delta)./(4*pi*D*d);
     Mil = m(i,3);
     Mair = m(i,4);
     G(i,2) = T/(Mil/Mair);
     plot(i,G(i,2),'b+')
end

xlabel('probe #')
ylabel('G')
title('G factors for red (o) and infrared (+) for 24 probes')
axis([0 25 0 2])

%%%%%
% Calculate means and standard deviations
% ignoring probe #2
%%%
['      mean    std dev']
Gred = [G(1,1) G(3:24,1)'];
red = [mean(Gred) std(Gred)]

Gir = [G(1,2) G(3:24,2)'];
ir = [mean(Gir) std(Gir)]
```

FIG. 8

```
% grid.m

clear

%%%%%%%
% Load nm(), oxyblood(), deoxyblood(), bloodless(),
%       musp_dermis(), musp_blood()  for 250:2:1000 nm =
(1:376).
% Retain only the optical properties at 730 and 940 nm.
%%%%
tissueoptics
i730 = 241;                           % index: nm(i_730) = 730
i940 = 346;                           % index: nm(i_940) = 940
oxy(1:2) = [oxyblood(i730) oxyblood(i940)];
deoxy(1:2) = [deoxyblood(i730) deoxyblood(i940)];
skin(1:2) = [bloodless(i730) bloodless(i940)];
musp_skin(1:2) = [musp_dermis(i730) musp_dermis(i940)];
musp_bl(1:2) = [musp_blood(i730) musp_blood(i940)];
clear nm oxyblood deoxyblood bloodless musp_dermis
musp_blood;

figure

for i = 1:21
      fv = (i-1)*0.01;   % choose series of blood volume
fractions
      fvbl(i) = fv;
      for j = 1:11
            SmO2 = (j-1)/10;    % choose series of SmO2 values
            SO2(j) = SmO2;
            mua_mixed    = fv*( SmO2*oxy + (1-SmO2)*deoxy ) +
(1-fv)*skin;
            musp = fv*musp_bl + (1-fv)*musp_skin;
            optprops = [musp mua_mixed];
            result = calcDC(optprops);
            Tred(i,j) = result(1);
            Tir(i,j) = result(2);
      end % j
end % i
plot(Tred, Tir, 'c-')
hold on

for i = 1:21
      plot(Tred(i,:),Tir(i,:),'c-')
end

xlabel('Tred')
ylabel('Tinfrared')
title('T_red and T_ir grid vs SmO2 and fv')
axis([0 3 0 1])
```

FIG. 9

```
% calcDC.m

function DC = calcDC(optprops)

musp = optprops(1:2);
mua_mixed = optprops(3:4);

d = 0.55;

for j=1:2 . % 1=red, 2=infrared

mua = mua_mixed(j);
D = 1/(mua + musp(j))/3;
delta = sqrt(D/mua);
DC(j) = exp(-d/delta)/(4*pi*D*d);

end %j
```

FIG. 9A

INTERNATIONAL SEARCH REPORT

International application No.

PCT/US00/19293

A. CLASSIFICATION OF SUBJECT MATTER

IPC(7) :A61B 5/00
US CL :600/331

According to International Patent Classification (IPC) or to both national classification and IPC

B. FIELDS SEARCHED

Minimum documentation searched (classification system followed by classification symbols)

U.S. : 250/252.1; 600/323, 330, 331, 336

Documentation searched other than minimum documentation to the extent that such documents are included in the fields searched

Electronic data base consulted during the international search (name of data base and, where practicable, search terms used)

C. DOCUMENTS CONSIDERED TO BE RELEVANT

Category*	Citation of document, with indication, where appropriate, of the relevant passages	Relevant to claim No.
A	US 4,892,101 A (CHEUNG et al.) 09 January 1990, entire document.	1-21

☐ Further documents are listed in the continuation of Box C. ☐ See patent family annex.

*	Special categories of cited documents:	"T"	later document published after the international filing date or priority date and not in conflict with the application but cited to understand the principle or theory underlying the invention
"A"	document defining the general state of the art which is not considered to be of particular relevance		
"E"	earlier document published on or after the international filing date	"X"	document of particular relevance; the claimed invention cannot be considered novel or cannot be considered to involve an inventive step when the document is taken alone
"L"	document which may throw doubts on priority claim(s) or which is cited to establish the publication date of another citation or other special reason (as specified)	"Y"	document of particular relevance; the claimed invention cannot be considered to involve an inventive step when the document is combined with one or more other such documents, such combination being obvious to a person skilled in the art
"O"	document referring to an oral disclosure, use, exhibition or other means		
"P"	document published prior to the international filing date but later than the priority date claimed	"&"	document member of the same patent family

Date of the actual completion of the international search	Date of mailing of the international search report
19 SEPTEMBER 2000	18 OCT 2000
Name and mailing address of the ISA/US Commissioner of Patents and Trademarks Box PCT Washington, D.C. 20231 Facsimile No. (703) 305-3230	Authorized Officer ERIC F. WINAKUR Telephone No. (703) 308-3940

Form PCT/ISA/210 (second sheet) (July 1998)*